International Journal of Mineral Processing 99 (2011) 61–69

Contents lists available at ScienceDirect

International Journal of Mineral Processing

journal homepage: www.elsevier.com/locate/ijminpro

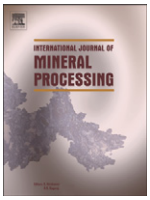

Effect of agitation on the settling behaviour of electrocoagulated silica

Roy O. Ifill [a,*], Thomas H. Etsell [b]

[a] Department of Civil & Environmental Engineering, 3-017 Markin/CNRL Natural Resources Engineering Facility, University of Alberta, 9105-116 Street, Edmonton, Alberta, Canada T6G 2W2
[b] Department of Chemical and Materials Engineering, 7th Floor, ECERF, University of Alberta, 9107-116 Street, Edmonton, Alberta, Canada T6G 2V4

ARTICLE INFO

Article history:
Received 16 October 2010
Received in revised form 10 February 2011
Accepted 10 April 2011
Available online 15 April 2011

Keywords:
Alternating current electrocoagulation
Agitation
Fine silica
Initial settling rate
Zeta potential
Floc growth

ABSTRACT

In conventional thickening operations, chemical reagents are added as coagulants or flocculants to improve the settling behaviour of suspended and colloidal solids. The effectiveness of these reagents depends on the nature and particle size of the solids. Poor settling may necessitate impoundment of the entire suspension, making land requirements exorbitant and imposing severe constraints on the plant water balance. The demand for fresh water increases as recycle of supernatant water from the thickening operation is curtailed. A bottleneck is created and plant capacity is effectively limited.

In light of these considerations, alternating current electrocoagulation (AC/EC) came to be viewed as a potential alternative to chemical coagulation for treating suspensions produced in the mineral, coal and petroleum industries. Consequently, a detailed program of fundamental study was undertaken on the application of AC/EC to the enhancement of the settling behaviour of fine silica, which served as the model tailings solid.

This paper reports on the study of the influence of agitation on the settling behaviour of silica that was treated by the AC/EC technique. The technique enhanced the initial settling rate of silica (1.6×10^{-3} cm/min) by over three orders of magnitude. Agitation was beneficial, but not essential, to this enhancement. Over the impeller tip speed range of 0 to 4.97 m/s, the initial settling rate of electrocoagulated silica was observed to be modestly sensitive to agitation rate, from which it may be deduced that silica formed strong flocs. Enhanced settling behaviour of electrocoagulated fine particles is manifested by their aggregation into flocs, as well as by their adsorption onto larger particles. In comparison tests, all of the aluminum added in chemical coagulation was precipitated in the sweep floc mechanism. This was not the case in electrocoagulation, which produced less voluminous sediment for the same Al dosage. In coagulation by specific adsorption, such as in electrocoagulation, zeta potential cannot be relied upon to track the progress of particle destabilization.

1. Introduction

1.1. Background

The dewatering behaviour of tailings directly affects the utilization of a tailings pond, which is designed principally as a repository for the solids, while permitting recycle of the supernatant water to the process plant. A major requirement for efficient operation is that the solids settle readily in the tailings pond. Poorly settling solids, therefore, severely restrict water recycle and impose an exorbitant demand on land space for storage of the tailings slurry. Concomitantly, the demand for make-up water increases.

Poor settling of particulates in aqueous media arises from mutual repulsion of the surface charge on the particles. Neutralization of the charge, the generation of precipitate to enmesh and sweep out the suspended particles, and the creation of interparticle bridges are mechanisms by which settling behaviour is enhanced. Chemical coagulants or flocculants are traditionally added to effect enhancement by these mechanisms. Alternatively, the coagulants may be generated *in situ* by electrolytic means (*i.e.*, electrocoagulation) as hydroxoaluminum complexes, under the influence of either direct current (DC) or alternating current (AC). In this study, alternating current electrocoagulation (AC/EC) was applied to enhance the settling behaviour of fine silica as the model tailings solid. Aluminum was selected as the material for electrode construction.

AC/EC was preferred in this study to DC/EC for practical reasons. AC/EC can be powered directly from the mains, requiring only a transformer to regulate the current, as was done in this study. DC/EC, on the other hand, can be powered by a battery for laboratory purposes, with a rheostat for current adjustment. For larger scale application, however, AC power would be the practical choice and rectifiers would be required to convert it to DC. It appears, therefore, that the operation of DC/EC on a commercial scale would incur higher capital expenditure than AC/EC, mainly for ancillary electrical equipment.

---

* Corresponding author. Tel.: +1 780 492 1436; fax: +1 780 492 8198.
E-mail addresses: ifill@ualberta.ca (R.O. Ifill), tom.etsell@ualberta.ca (T.H. Etsell).

0301-7516/$ – see front matter © 2011 Elsevier B.V. All rights reserved.
doi:10.1016/j.minpro.2011.04.004

1.2. Hydroxoaluminum complexation

The polarity of the electrodes reverses once per AC cycle such that each electrode functions alternately as the anode and as the cathode. The desired reaction occurring at the anode is the oxidation of aluminum (Eq. (1)):

$$\mathrm{Al(s)} \rightarrow \mathrm{Al}^{3+} + 3\mathrm{e} \tag{1}$$

Depending on the water pH, anodic side reactions may occur to liberate oxygen as shown in Eqs. (2) and (3).

$$2\mathrm{H_2O}(\ell) \rightarrow 4\mathrm{H}^+ + \mathrm{O_2(g)} + 4\mathrm{e} \quad \text{(neutral to acidic pH range)} \tag{2}$$

$$4\mathrm{OH}^- \rightarrow 2\mathrm{H_2O}(\ell) + \mathrm{O_2(g)} + 4\mathrm{e} \quad \text{(basic pH range)} \tag{3}$$

The reaction in Eq. (1) is not reversed at the cathode for the same reason that aluminum cannot be electrowon from aqueous solution. Instead, the cathodic reactions depend on pH and aeration, as indicated by Eqs. (4)–(7).

$$2\mathrm{H_2O}(\ell) + 2\mathrm{e} \rightarrow \mathrm{H_2(g)} + 2\mathrm{OH}^- \quad \text{(neutral to basic pH range; unaerated)} \tag{4}$$

$$2\mathrm{H}^+ + 2\mathrm{e} \rightarrow \mathrm{H_2(g)} \quad \text{(acidic pH range; unaerated)} \tag{5}$$

$$2\mathrm{H_2O}(\ell) + \mathrm{O_2(g)} + 4\mathrm{e} \rightarrow 4\mathrm{OH}^- \quad \text{(neutral to basic pH range; aerated)} \tag{6}$$

$$4\mathrm{H}^+ + \mathrm{O_2(g)} + 4\mathrm{e} \rightarrow 2\mathrm{H_2O}(\ell) \quad \text{(acidic pH range; aerated)} \tag{7}$$

Al^{3+} enters complexation reactions with water to form a range of hydroxo species (Baes and Mesmer, 1976; Cañizares et al., 2006), such as $Al(OH)^{2+}$, $Al(OH)_2^+$, $Al(OH)_3^o$, $Al(OH)_4^-$, $Al_2(OH)_2^{4+}$ and $Al_3(OH)_4^{5+}$. The relative abundances of these species are determined mainly by pH and the total concentration of dissolved aluminum. Ageing and temperature also determine the distribution and identity of the species (Stumm and O'Melia, 1968). Some polynuclear species are considered to form by condensation of the mononuclear hydrolysis products (Dentel and Gossett, 1988; Parthasarathy and Buffle, 1985; Snoeyink and Jenkins, 1980), as summarized by Eqs. (8) and (9) where the role of coordinated water molecules is evident.

$$\mathrm{Al(H_2O)_6^{3+}} \leftrightarrows \mathrm{Al(H_2O)_5OH^{2+}} + \mathrm{H}^+ \tag{8}$$

$$2\mathrm{Al(H_2O)_5OH^{2+}} \leftrightarrows \mathrm{Al_2(H_2O)_8(OH)_2^{4+}} + 2\mathrm{H_2O}(\ell) \tag{9}$$

The oxyhydroxoaluminum species, $Al_{13}O_4(OH)_{24}^{7+}$ (Baes and Mesmer, 1976; Akitt and Farthing, 1978), and other polynuclear species, such as $Al_7(OH)_{17}^{4+}$ and $Al_{13}(OH)_{34}^{5+}$ (Snoeyink and Jenkins, 1980), were identified. More recently, by mass spectrometric analysis of $AlCl_3$ solutions (pH 3.27 to 4.20), Sarpola et al. (2004) identified over 80 univalent cations (Al_2 to Al_{13} cores) and 19 polyvalent cations (Al_{10} to Al_{27} cores). While it had been well established (*e.g.*, Baes and Mesmer, 1976; Duan and Gregory, 2003) that the aluminate ion was the only known complex anion of aluminum, Sarpola et al. further identified 45 univalent anions (Al_1 to Al_{12} cores) and 9 polyvalent anions (Al_{10} to Al_{32} cores). Thus, the inference drawn by Hunt (1965) and Stol et al. (1976), that there might be a practically infinite range of hydrolytic aluminum complexes, was proven. The identity and distribution of the species change with pH, total dissolved aluminum concentration, and time (*i.e.*, age) (Sarpola et al., 2006; Zhao et al., 2009).

The hydroxoaluminum and oxyhydroxoaluminum ions adsorb specifically (*i.e.*, chemisorb) onto particle surfaces and neutralize charge residing there. Consequently, interparticle repulsion is reduced or eliminated, permitting closer approach and contact of particles to form aggregates or flocs. Furthermore, the adsorbed complexes can continue to adsorb onto other particles with which their host particles make contact, creating and building flocs by effectively bridging particles to particles, particles to microflocs, and microflocs to microflocs.

1.3. Agitation and floc growth

Interparticle collision, and collision between particles and coagulant species, are prerequisite to the formation of flocs which, by their mass and structure, dewater and settle more readily than the individual particles. The collisions are facilitated by agitation, whose effect on the settling behaviour of electrocoagulated silica is the subject of this paper. Aluminum ion formation and complexation are not influenced by agitation.

In their study of the flocculation of ground silica ($d_{50} = 24\ \mu m$) with Armac C™ (a flotation collector) under shear, Spears and Stanley (1994) identified two stages of floc growth. They found that flocculation began with rapid floc growth, followed by the attainment of a steady state between growth and fragmentation. The limiting floc size was determined by the hydrodynamic conditions and the flocculant dosage. At zero flocculant dosage, flocculation did not occur at any agitation rate. In addition, the agitation rate producing the largest flocs decreased as the solids concentration was increased. This result indicated that the closer proximity of the silica particles, due to increasing concentration, resulted in higher collision frequency which enhanced the flocculation process. The result also illustrated that the flocs would fragment when subjected to excessive shear rates. Once the limiting floc size was attained, however, no significant net fragmentation resulted from prolonged agitation.

It must be pointed out that the work of Spears and Stanley (1994) was a study of the shear-flocculation phenomenon previously described by Warren (1975). In shear-flocculation, hydrophobic surfactant adsorbs onto the solid particles. By the energy available from high shear rates, the particles collide and aggregate in hydrophobic–hydrophobic association. Such aggregates exhibit high shear strength because of the high binding energy required to form them. Warren (1975) estimated the binding energy per particle–particle contact to be of the order of $(10^3–10^4)kT$ J, where k is Boltzmann's constant (1.381×10^{-23} J/°K) and T is the absolute temperature (°K). This is to be compared with ~10kT J for polymer-bridging flocculation. Hence, the nature of shear-flocculation differs significantly from that of chemical flocculation. Furthermore, it will be shown in the current paper that floc formation by electrocoagulation proceeded in the absence of shear. Hence, the nature of electrocoagulation is also very different from that of shear-flocculation.

It is interesting to note that Spears and Stanley (1994) achieved flocculation at a zeta potential of −26 mV. This is not unusual since coagulation and flocculation can be achieved well before charge neutralization occurs (Cohen and Hannah, 1971). In flocculation with flocculants of high molecular weight, for instance, the polymer bridge can be much longer than the thickness of the electrical double layer. Hence, no effect is likely to be seen on the measured value of the zeta potential.

In another study of ground silica ($d_{50} = 28\ \mu m$), Sharma et al. (1994) used Percol 351™ as the flocculant. It was added continuously at two dosing rates to give a fixed dosage. Agitation was continued after the required dosage had been met. The floc size and growth rate were observed to increase with the flocculant dosing rate. At both dosing rates studied, doubling the shear rate almost halved the maximum floc size attained. After attainment of the maximum floc size, floc growth and fragmentation proceeded in steady state, and further flocculant addition had no incremental effect on floc size.

1.4. Silica surface chemistry

Hunter (1981) placed the isoelectric point (i.e.p.) of aged α-SiO_2 at pH 2.0 ± 0.3 and estimated the point of zero charge (p.z.c.) for quartz to be pH 2 to 3.7, while Lyklema (1978) quoted the value of the p.z.c.

for silica at pH ~ 2. These values attest to the acidic nature of silica. Consequently, the following equilibria have been proposed as possible surface reactions (Amirtharajah and O'Melia, 1990; Huang, 1981; Lyklema, 1978), where ≡Si represents a silicon surface atom.

$$\equiv\text{SiOH} \leftrightarrows \equiv\text{SiO}^{-} + \text{H}^{+}$$

$$\equiv\text{SiOH} + \text{OH}^{-} \leftrightarrows \equiv\text{Si(OH)}_2^{-}$$

$$\equiv\text{SiOH} + \text{H}^{+} \leftrightarrows \equiv\text{SiOH}_2^{+}$$

$$\equiv\text{SiOH} \leftrightarrows \equiv\text{Si}^{+} + \text{OH}^{-}$$

The capacity of the aluminum hydroxo complexes for interparticle bridging depends upon the magnitude of the charge carried by the complexes, as illustrated by Reactions 10 to 12. Reactions 10 and 11 exemplify a tetravalent dimeric complex with a large capacity for bridging, unlike the univalent monomeric complex in Reaction 12.

$$\equiv\text{Si}-\text{OH} + \text{Al}_2(\text{OH})_2^{4+} \leftrightarrows \equiv\text{Si}-\text{OAl}_2(\text{OH})_2^{3+} + \text{H}^{+} \qquad (10)$$

$$\equiv\text{Si}-\text{OAl}_2(\text{OH})_2^{3+} + \text{HO}-\text{Si}\equiv \leftrightarrows \equiv\text{Si}-\text{OAl}_2(\text{OH})_2^{2+}-\text{O}-\text{Si}\equiv + \text{H}^{+} \qquad (11)$$

$$\equiv\text{Si}-\text{OH} + \text{Al(OH)}_2^{+} \leftrightarrows \equiv\text{Si}-\text{OAl(OH)}_2 + \text{H}^{+} \qquad (12)$$

Thus, like the dimer in Eq. (10), $\text{Al}_{13}\text{O}_4(\text{OH})_{24}^{7+}$, $\text{Al}_7(\text{OH})_{17}^{4+}$ and $\text{Al}_{13}(\text{OH})_{34}^{5+}$ would be examples of complexes that possess great capacity for interparticle bridging, for effecting floc growth and, ultimately, for enhancing the settling behaviour of fine particulate solids.

2. Materials and methods

2.1. Characterization of As-received silica

The silica was supplied under the trade name, Sil-Co-Sil Ground Silica, by the Ottawa Silica Company of Ottawa, Illinois, USA, and was tested as received. It was characterized by its moisture content, density and particle size distribution. In addition, its zeta potential and natural settling behaviour were determined in de-ionized water containing 0 and 200 mg/L (200 mg/dm^3) NaCl (reagent grade, added to increase the specific conductivity for electrocoagulation).

As set out in Standard D 422 (ASTM, 1997), the hydrometer method was used to determine the particle size distribution of as-received silica. De-ionized water was used instead of distilled water. The hydrometer had a cylindrical bulb and was graduated over the specific gravity range of 0.995 to 1.300.

The natural settling behaviour of as-received silica was established by the timed, downward movement of the solid–liquid interface in a graduated cylinder. Zeta potential was measured in de-ionized water containing 0 and 200 mg/L NaCl over the pH range of 3.0 to 9.3. A Rank Brothers micro-electrophoresis unit Mark II was used with a flat electrophoresis cell. At each stationary position, the time taken for each of 10 particles to traverse 100 μm was recorded. The particles were timed successively in opposite directions of travel to minimize electrode polarization. The ratio of the cell dimensions (ℓ/d) was 9.64, where ℓ represents the internal height of the cell, and d the internal width of the cell. For the location of the stationary positions in the cell, the Komagata correction for $\ell/d<20$ was invoked, as instructed by Rank Brothers (1986) and as rationalized by Hunter (1981).

2.2. De-ionized water

De-ionized water was prepared from tap water with a Barnstead D8902 cartridge of mixed resin. It was used as wash water and as the dispersion medium for silica.

Temperature and pH were measured with a Cole Parmer Chemcadet Model 5986-60 combination pH/ORP (oxidation–reduction potential) meter. Temperature readings were occasionally checked against those of a mercury-in-glass thermometer. The pH meter was calibrated against standard buffers supplied by Fisher Scientific.

The absolute viscosity of de-ionized water and of de-ionized water containing 200 mg/L NaCl was measured to facilitate determination of the zeta potential and particle size distribution of as-received silica. The viscosity was measured with a Cannon Fenske routine viscometer, No. 50-M309, as prescribed in Standards D 445 and D 446 (ASTM, 1996).

2.3. Electrocoagulation apparatus

The electrodes were 0.7 mm thick rectangular plates measuring 22 cm × 20 cm and were fabricated from 6061-T6 aluminum alloy. Electrocoagulation was performed in the 5.7-L Plexiglas™ cell sketched in Fig. 1. Two spigots (not shown in the diagram), each equipped with a sample cock, were fitted at X and at Y to facilitate sampling of the supernatant water and electrocoagulated slurry, respectively. The electrodes were held snugly in 1-mm wide grooves that were cut 0.5 cm apart along the top edge of one end wall of the cell and along a removable Plexiglas™ bridge placed near the other end wall. The bridge itself was slotted near its ends to ride the side walls of the cell. A Plexiglas™ comb was placed on the base of the cell in contact with the grooved end wall. The bottom edges of the electrodes fitted snugly into the grooves of the comb to maintain a constant electrolytic area of 299.1 cm^2, as well as to prevent contact between electrodes when agitation was applied. An overhead motor powered a Teflon™-coated paddle assembly which incorporated an axial-flow impeller, 5 cm in diameter.

2.4. AC/EC test procedures

In the preparation of feed water, 800 mg of NaCl was dissolved in 4.0 L of de-ionized water. The temperature of the resulting solution was adjusted and noted. The electrodes were installed in the cell and connected to the power supply (Fig. 2) with a variable transformer by which the output voltage and, hence, the current to the electrocoagulation cell were controlled. The transformer was a Powerstat™ Model 136B from The Superior Electric Co. of Bristol, Connecticut, USA. A current transformer (not shown) enabled the magnitude of the current

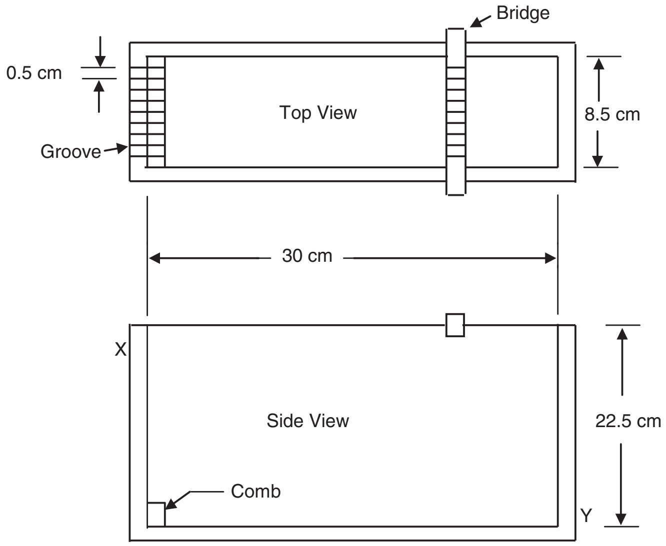

Fig. 1. Sketch of the electrocoagulation cell.

to be displayed digitally by a Novatron™ ammeter. A Novatron™ voltmeter indicated the AC voltage in digital readout.

In preparation for electrocoagulation, 210.5 g of as-received silica was dispersed in the 4.0 L of feed water in the cell to a concentration of 5.0 wt.% solids. After the suspension temperature and pH had been recorded, the current flow (at a density of 70.2 A/m^2) and timing were started, the current being maintained by continual manual adjustment of the voltage. As electrocoagulation proceeded, the suspension temperature and the applied voltage were recorded every minute. The silica suspension was electrocoagulated in four tests, with and without agitation, for 30 and 75 min. When agitation was applied, the impeller tip speed was 1.73 m/s. This mode of agitation was preferred to bubbling air (Parekh et al., 1992) because it was easily controlled and it gave reproducible results.

At the end of the electrocoagulation time, the current flow was stopped and the electrodes, bridge and comb were removed. A sample of the electrocoagulated slurry was retained for examination of the floc morphology. After every test, the electrodes were cleaned with fine steel wool, washed with tap water, and rinsed with acetone for quick drying.

2.5. Agitation rate tests

The influence of agitation on floc formation and settling was investigated further over a range of continuous agitation rates, which were defined by the impeller tip speed. Six tests were performed over the full range of agitator motor speed which gave a maximum impeller tip speed of 4.97 m/s. In these electrocoagulation tests, current at a density of 70.2 A/m^2 was passed for 30 min between two electrodes positioned 3.0 cm apart.

2.6. Settling test procedure

After AC/EC treatment, 1 L of electrocoagulated slurry was withdrawn under continuous agitation and subjected to a 60-minute settling test at 24 °C in a graduated cylinder. Enhancement in settling behaviour was evaluated by comparison of initial settling rates.

2.7. Examination of floc morphology

One drop of a selected suspension or slurry sample was placed on a glass slide and covered carefully with a small, thin glass cover-slip. The particles were viewed on a confocal scanning electron microscope (Molecular Dynamics, Multipro 2001) which used an Ar/Kr laser as the light source with phase contrast imaging.

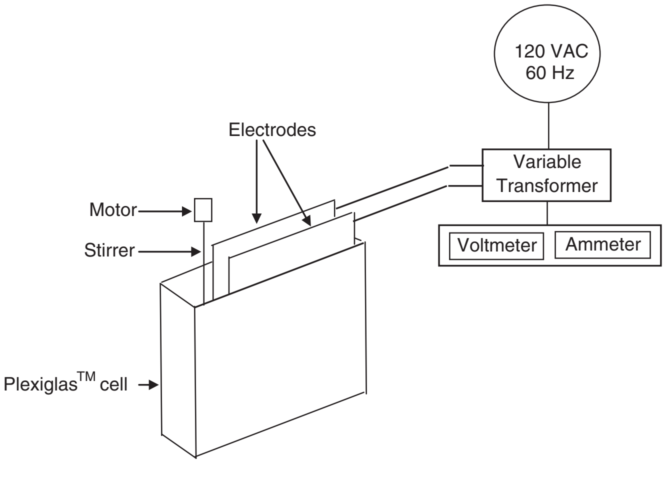

Fig. 2. AC/EC apparatus.

2.8. Preparation and identification of aluminum cations

The AC/EC procedure differed here from that in Section 2.4. A 3.2 A current was passed for 30 min between two electrodes immersed in 4.0 L of de-ionized water containing 20 mg/L NaCl. This concentration was preferred to 200 mg/L because the latter obscured the aluminum species. The total dissolved Al concentration was about 10 mg/L. Agitation was continuous (impeller tip speed, 1.75 m/s) during AC/EC treatment of the feed water. After treatment, 52.63 g of as-received silica was slurried with 1.0 L of AC/EC-treated water, which contained aluminum hydroxide precipitate formed during AC/EC treatment. Samples of feed water, AC/EC-treated water (minus precipitate) and supernatant water were submitted for identification of aluminum cationic species.

Qualitative mass spectrometric analysis was performed in positive mode of electrospray ionization on a Micromass ZabSpec Hybrid Sector-TOF. The samples were infused into the electrospray source with a Harvard syringe pump at a flow rate of 10 μL/min. Prepurified nitrogen served as a spray pneumatic aid and bath gas at approximately 80 °C (to evaporate water from the atomized samples). The mass spectrum was acquired by full magnetic scan over the range of 10 to 1000 Da (*i.e.*, ionic mass-to-charge ratios, m/z, of 10 to 1000) at a rate of 10 s/decade. Data acquisition and processing were achieved by an OPUS software package on a Digital Alpha station with VMS operating system.

2.9. Jar test procedure

As-received silica was coagulated with alum, $Al_2(SO_4)_3{\bullet}18H_2O$, and with aluminum chloride, $AlCl_3{\bullet}6H_2O$, in jar tests for comparison with electrocoagulation. Since a 5.0 wt.% silica suspension is much denser than raw water, the agitator speeds suggested by the American Water Works Association procedure (1977) had to be increased considerably.

The silica was dispersed in 800 to 900 mL of de-ionized water at 22 °C in a 1-L beaker under continuous agitation at 800 r.p.m. (tip speed 2.09 m/s). The paddle assembly was the same as that used in the electrocoagulation studies. Two 13-mm wide polyethylene baffles were installed in the beaker to ensure good mixing while preventing splashing. The baffles were positioned diametrically opposite each other, with a space of about 2 mm from the beaker wall and bottom to prevent accumulation of the solids. After the temperature and pH of the suspension had been measured, a quantity of sodium carbonate was dissolved in de-ionized water and added to the beaker. The mass of Na_2CO_3 was calculated to neutralize the acid that would be formed by hydrolysis of the aluminum salt, which would be added subsequently (see Reactions 13 to 15 where "am" means "amorphous"). After the suspension pH had stabilized, it was measured together with the suspension temperature.

$$Al^{3+} + 3H_2O \rightarrow Al(OH)_3(am) + 3H^+ \quad (Al^{3+}\ \text{hydrolysis}) \tag{13}$$

$$3H^+ + 3CO_3^{2-} \rightarrow 3HCO_3^- \quad (\text{acid neutralization}) \tag{14}$$

$$Al^{3+} + 3H_2O + 3CO_3^{2-} \rightarrow Al(OH)_3(am) + 3HCO_3^- \quad (\text{overall reaction}) \tag{15}$$

A mass of the aluminum salt, which was calculated for a predetermined dosage (ranging from 10 to 100 mg/L Al), was dissolved in a volume of de-ionized water that complemented the 1.00 L required for the 52.63 g of silica dispersed at the beginning. The aluminum salt solution was added quickly to the suspension and timing started. After 1 min, the impeller speed was reduced to 650 r.p.m. (tip speed 1.70 m/s) and maintained for an additional 20 min. These times were the same as those employed by Dentel and Gossett (1988) to coagulate silica. The coagulated slurry was subjected to a settling test at 24 °C, after which the supernatant was sampled for analysis of total aluminum.

2.10. Total aluminum analysis

In preparation for analysis, one drop of concentrated HCl was added to each sample (~60 mL) to prevent precipitation of aluminum hydroxide. A similar addition was made to a blank sample of feed water. Analysis was performed by atomic absorption spectrophotometry on a Perkin Elmer 4000 double beam analyzer.

3. Results and discussion

3.1. Characteristics of As-received silica

The as-received silica had a density of 2534.8 kg/m^3 and was thoroughly dry (<0.01% moisture). The d_{50} was 20 μm and the top size was about 65 μm. Approximately 6% had an equivalent diameter of ≤1 μm.

The silica exhibited poor settling behaviour in de-ionized water (no NaCl addition), requiring 17.2 h to settle by 1.0 cm. This is equivalent to an initial settling rate of 9.7×10^{-4} cm/min. In de-ionized water containing 200 mg/L NaCl, the initial settling rate was practically the same at 1.6×10^{-3} cm/min. Hence, the 200 mg/L NaCl addition did not destabilize the suspension. Therefore, any significant enhancement in settling behaviour observed after electrocoagulation would be entirely attributable to the AC/EC process. At the time the natural settling behaviour of silica was observed, the supernatant was clear just below the meniscus, merging into a narrow region of pure colloidal dispersion which had a gelatinous appearance. Below this region, a stable suspension prevailed, such that the sludge line (*i.e.*, the interface between the settled solids and the suspension) was indistinguishable.

The effects of pH and NaCl concentration on the zeta potential of silica are illustrated in Fig. 3. The zeta potential was negative over the pH range studied (3.0 to 9.3) and increased negatively with rising pH by the surface reaction in Eq. (16) (Letterman et al., 1982; Stumm, 1992; Elzo et al., 1998).

$$\equiv\mathrm{Si-OH} + \mathrm{OH}^- \leftrightarrows \equiv\mathrm{Si-O}^- + \mathrm{H_2O} \qquad (16)$$

The addition of electrolytes is known (*e.g.*, Elzo et al., 1998) to lower (*i.e.*, make less negative) the zeta potential of silica as the electrical diffuse layer is compressed. However, the results of the current study show that the addition of 200 mg/L (3.4 mM) NaCl raised (*i.e.*, made more negative) the zeta potential (Fig. 3). This observation agrees with the results of Riddick's (1968) investigation in which the incremental addition of NaCl increased the zeta potential from −30 mV (1 mg/L NaCl) to −50 mV (200 mg/L NaCl). It was only after approximately 500 mg/L NaCl had been added that the zeta potential began to decrease (*i.e.*, became less negative), consistent with the known effect of electrolyte addition.

The i.e.p. would be expected to occur around pH 2 (Fig. 3). In the presence of 200 mg/L NaCl, the zeta potential increased sharply when the pH exceeded 8.7, probably due to the surface reaction in Eq. (16) combined with the participation of Cl$^-$, as suggested by Eq. (17).

$$\equiv\mathrm{Si-OH} + \mathrm{Cl}^- + \mathrm{OH}^- \leftrightarrows \equiv\mathrm{Si-OCl}^{2-} + \mathrm{H_2O} \qquad (17)$$

3.2. Effects of agitation

Fig. 4 depicts the enhanced settling behaviour of the electrocoagulated silica and the effect of agitation at two AC/EC retention times. Thirty minutes' electrocoagulation enhanced the settling behaviour of silica, such that initial settling was completed within 8 min, followed by about 20 min of compression. Agitation had a much greater effect on the degree of settling enhancement in 75 minutes' electrocoagulation than in 30 minutes'. Initial settling ended within 4 min and was followed by about 10 min of compression. Hence, the silica electrocoagulated for 75 min under continuous agitation had finished settling within 15 min.

The significance of the relative displacement of the curves in Fig. 4 can be assessed by inspection of the initial settling rates in Table 1. The initial settling rates ranged from 4.3 to 8.0 cm/min, representing over three orders of magnitude enhancement relative to the natural settling rate (1.6×10^{-3} cm/min). The benefit of agitation is apparent, especially after the longer electrocoagulation time: agitation enhanced the initial settling rate further by 11.6% (30 min) and 73.9% (75 min). It is concluded, therefore, that agitation is desirable, but not essential, for AC/EC to be effective in enhancing the settling behaviour of silica. It is interesting to note that electrocoagulation for 30 min under continuous agitation and for 75 min without agitation produced the same degree of enhancement of the initial settling rate. Hence, agitation can shorten the electrocoagulation time required to achieve a given initial settling rate. Alternatively, it can be deduced that the initial settling rate of silica is enhanced more rapidly with increasing electrocoagulation time when agitation is applied than when it is not.

Fig. 5 shows photomicrographs of: (a) discrete particles of as-received silica; (b) silica flocs formed in 30 minutes' electrocoagulation under quiescent conditions; and (c) silica flocs formed in 30 minutes' electrocoagulation under continuous agitation. The silica particles were angular, and the absence of any aggregation in the as-received material is apparent in Fig. 5a. Fig. 5b and c illustrate the difference in character or texture of the flocs, which appear as dark or

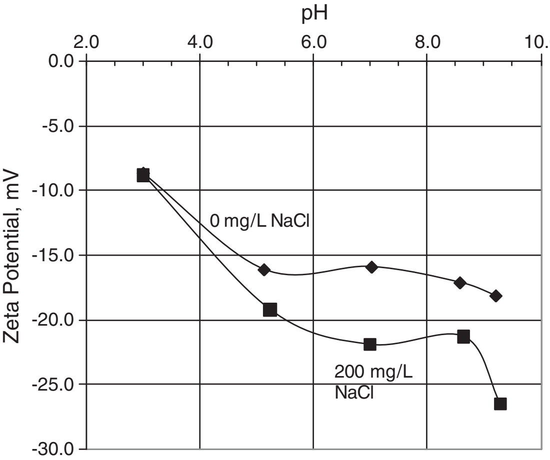

Fig. 3. Zeta potential of as-received silica.

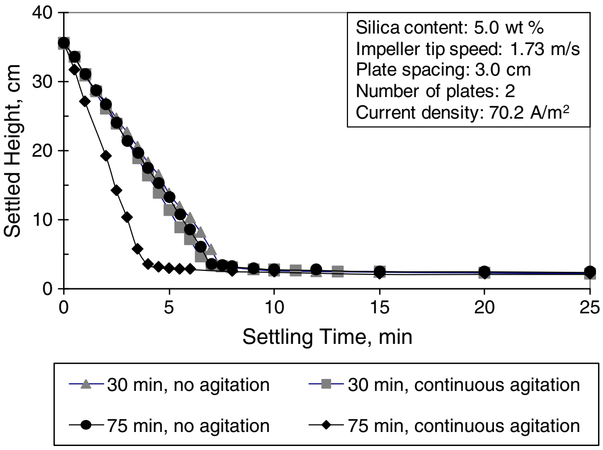

Fig. 4. Enhanced settling of electrocoagulated silica.

Table 1
Effect of agitation and AC/EC time on settling behaviour of silica.

AC/EC time (min)	Agitation	Initial settling rate (cm/min)	Temperature rise (°C)
30	No	4.3	10.2
30	Yes	4.8	8.9
75	No	4.6	18.3
75	Yes	8.0	17.1

(a) As received.

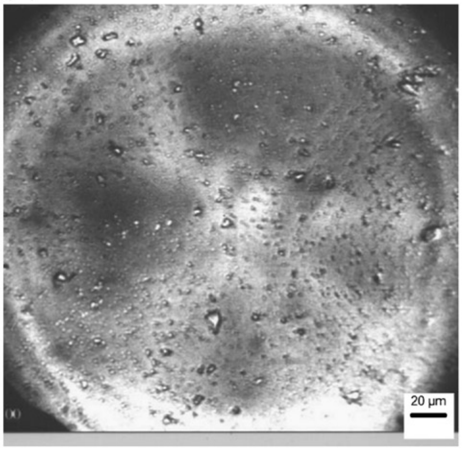

(b) AC/EC: 30 min, quiescent.
Pulp pH: feed, 8.63; treated, 8.57.

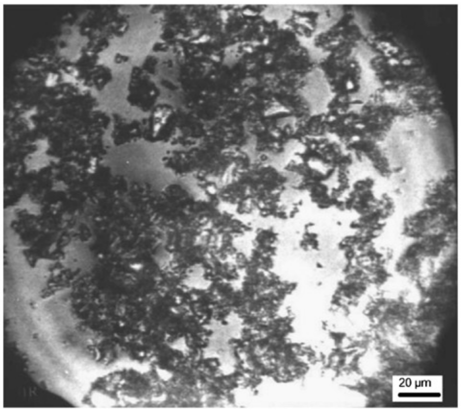

(c) AC/EC: 30 min, agitation.
Pulp pH: feed, 8.79; treated, 8.57.

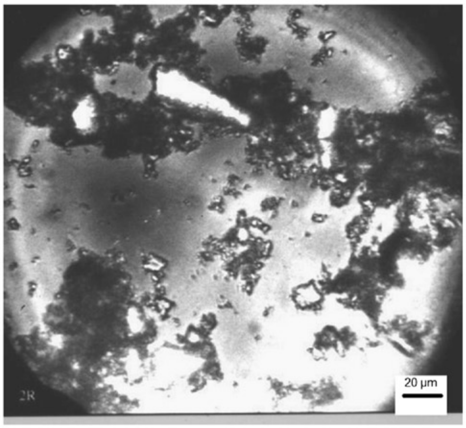

Fig. 5. Textures of as-received and electrocoagulated silica.

black masses and were formed under different agitation conditions. In the absence of agitation (Fig. 5b), the flocs adopted a fibrous, loose texture while, with agitation (Fig. 5c), the flocs appear more compact. In addition to floc size, the texture and morphology are expected to influence the settling behaviour of electrocoagulated silica. Bouyer et al. (2005) observed that the manner of floc development depends, in part, on the hydrodynamics (*e.g.*, agitation rate). Further, Coufort et al. (2005) reported that shear stress causes the floc size to decrease, making the floc structure more compact. Fig. 5b and c also show that the flocs were comprised of particles in a wide size range. The 55-μm particle in Fig. 5c can be observed to have small particles adsorbed onto its surfaces, even at the corners. Hence, the hydroxoaluminum complexes, which were formed during electrocoagulation, adsorbed onto the entire surface of the silica particles. Thus, the settling behaviour of fine particles is enhanced by direct adsorption onto large particles, as well as by aggregation into flocs.

The quiescent conditions prevailing in two of the tests enabled observation of the onset of enhanced settling behaviour, which commenced after about 8 min of electrocoagulation. As the AC/EC treatment progressed, the mud line (*i.e.*, the interface between the supernatant water and the electrocoagulated silica) became sharper.

The initial settling rates achieved after 30 minutes' electrocoagulation at impeller tip speeds of 0 to 4.97 m/s are plotted in Fig. 6. They indicate that the settling behaviour of electrocoagulated silica did not change significantly over the full range of agitation rates. Thus, the effectiveness of 30 minutes' AC/EC in enhancing the settling behaviour of silica was not greatly sensitive to agitation rate. The maximum initial settling rate of about 4.9 cm/min occurred in the tip speed range of 2.0 to 3.0 m/s. Hence, at higher impeller tip speeds, agitation became counterproductive. It is inferred that such agitation rates limited floc size. The impeller tip speed of 1.73 m/s was selected for subsequent tests because it eliminated the risk of splattering and its effect on the initial settling rate was virtually at its maximum.

These results suggest that, in an industrial application of the AC/EC technique, the continuous flow of suspension through the cell would be expected to provide adequate agitation. The redundancy of an agitator, therefore, represents a capital cost saving, as well as energy and maintenance cost savings.

3.3. Dispersion medium and suspension

Hydrogen was evolved (Jenke and Diebold, 1984; Pretorius et al., 1991; Vik et al., 1984) as tiny bubbles (≤0.5 mm in diameter) at the facing surfaces as the electrodes alternated duty as the cathode. In addition, these surfaces became pitted during the anode cycle. The pits, which were arrayed in the flow pattern of the suspension, developed as Al was oxidized to Al^{3+}, precursory to the formation of complex hydroxo species. Such species are capable of neutralizing the negative surface charge on the silica particles and of bridging the destabilized (*i.e.*, electrocoagulated) silica particles to form flocs (Black, 1967; Duan and Gregory, 2003; Hahn and Stumm, 1968; Stumm and Morgan, 1970; Trompette and Vergnes, 2009).

With increasing electrocoagulation time, the temperature of the suspension rose as a result of Joule heating (Table 1). The water conductivity also increased, necessitating continual reduction of the applied voltage.

For ready comparison, the electrocoagulated slurry and supernatant water samples were cooled to the initial temperature of the feed suspension before pH measurements were made. The pH of the electrocoagulated slurry tended to be slightly lower than that of the feed suspension, as Table 2 illustrates. In the quiescent 75-minute test, the feed suspension and electrocoagulated slurry had the same pH of

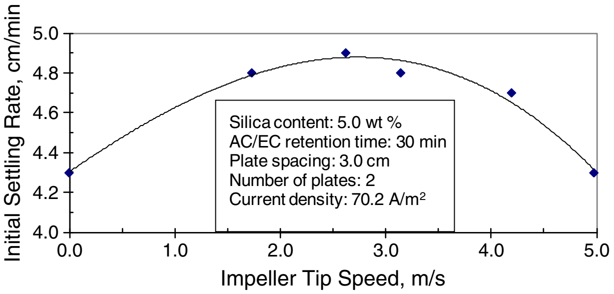

Fig. 6. Effect of agitation rate during AC/EC on silica settling behaviour.

8.70. In a subsequent paper, data from other tests will illustrate that, during electrocoagulation, the pH first falls and then rises. Hence, the value of the terminal pH depends on the AC/EC retention time and on the reactions that occur.

Water pH data are reported in Table 2. The dispersion of silica in the feed water resulted in a suspension whose pH was higher than that of the feed water. Reactions occurring during electrocoagulation caused the pH of the supernatant to be higher than that of the feed water. This suggests net H^+ adsorption at the silica surface or net OH^- release at the silica surface, as the following reactions show:

$$\equiv SiO^- + H^+ \leftrightarrows \equiv SiOH$$

$$\equiv SiO^- + H_2O \leftrightarrows \equiv SiOH + OH^-$$

3.4. Particle dynamics and floc growth

An important point arises from electrocoagulation in the absence of agitation. Normally, colloidal particles are considered to be the size fraction that is amenable to perikinetic coagulation (Masliyah, 1994; Montgomery, Consulting Engineers, Inc., 1985; Tambo, 1991). In the as-received silica, colloidal particles constituted only a minor fraction (~6%≤1 μm or ~32%<10 μm). Hence, in the quiescent electrocoagulation, gas evolution from the electrodes, thermal convection currents, and sedimentation of silica flocs and coarse particles created hydrodynamic disturbances from which interparticle collisions resulted. Yet, the entire mass of silica was electrocoagulated, as was evident from the sedimentation occurring in the cell, but the manner of electrocoagulation could be described neither as purely perikinetic nor as purely orthokinetic. Diffusion of the coagulative aluminum species is considered to have facilitated their specific adsorption onto the silica surface. Interparticle bridging is automatically implied. This leads to the postulation that, in the absence of applied agitation, the proximity of particles to one another facilitated collision for the achievement of electrocoagulation of silica dispersed at high concentration (5.0 wt.% in this case). In an assumed monodisperse suspension of spherical d_{50} particles, the average separation between as-received silica particles was estimated to be 54 μm. Relative to its diameter, therefore, a particle would not have far to travel to become bridged to its nearest neighbour. The implication of this is that no externally applied shear is necessary, and incidental hydrodynamic disturbances (gas bubble movement, *etc.*) listed above would adequately facilitate floc formation. Test results in Table 1 indicate that interparticle collisions induced by shear improved floc growth, particularly at extended retention times (*i.e.*, higher aluminum dosages). More importantly, however, the results demonstrate that, in the 30-minute tests, externally applied agitation did not promote a substantially superior initial settling rate.

Estimates of the collision rates, under quiescent and shear conditions, between aluminum ions and silica particles, and of interparticle collision rates under shear have been made, and it will be shown in another paper that not all of the dissolved aluminum was adsorbed by silica. Hence, the number concentration of complex aluminum ions increased with electrocoagulation time, promoting higher frequency of collision with silica particles and flocs. Of course, the number concentration of individual silica particles decreased as new flocs were formed and as existing flocs grew. The rate of floc growth by ion-particle and interparticle collisions is anticipated to be faster than the rate of formation of new flocs. The justification for this expectation is that the growing flocs present a larger surface which, statistically, would experience a higher collision frequency. Hence, the effect of agitation in doubling the ion-particle collision rate became more productive with longer electrocoagulation time, as corroborated by the initial settling rates for 75 minutes' electrocoagulation (Table 1).

Since transport of the bulk of the silica particles was not caused by Brownian motion or by the AC electric field under quiescent conditions, electrostatic attraction between aluminum complexes and silica particles is expected to have played an important role in floc formation and growth. Such attraction would also facilitate collision between a particle bearing aluminum adsorbate and one without.

3.5. Aluminum speciation

Peaks in the spectrum obtained for the feed water blank sample were discounted from the spectra generated by the AC/EC-treated and supernatant water samples. The pH values of the freshly prepared samples measured 8.40 (AC/EC-treated) and 8.17 (supernatant). Of the remaining peaks, those showing at least a relative intensity of 10% were interpreted within the allowable ±0.55 Da of the analyzed m/z ratio. All of the identified species were trivalent and contained NaCl in significant molar quantities. The presence of NaCl was indicated by lines for the two chlorine isotopes, $^{35}_{17}Cl$ and $^{37}_{17}Cl$. The identified aluminum species are listed in Table 3, which shows a trend of increasing molar quantities of NaCl associated with oxyhydroxoaluminum complexes of increasing molar mass. In contrast, the molar ratio of NaCl:Al^{3+} decreased with increasing size of the oxyhydroxo complexes: for example, from 1.06 for $[Al_3O(OH)_4(H_2O)_2 \cdot 3.18NaCl]^{3+}$ to 0.71 for $[Al_5O_2(OH)_8(H_2O)_7 \cdot 3.54NaCl]^{3+}$. For the hydroxoaluminum complexes containing coordinated water molecules, the NaCl:Al^{3+} molar ratio decreased as the molar mass of the complexes increased. However, unlike the trend observed for the oxyhydroxo complexes, the relation of NaCl molar content to the size of the complex is not readily

Table 2
Pulp and water pH.

AC/EC time (min)	Agitation	Temperature (°C)	Pulp pH		Water pH	
			Feed	Electrocoagulated	Feed	Supernatant
30	No	21.2	8.63	8.57	7.44	8.52
30	Yes	21.4	8.79	8.57	7.28	8.68
75	No	21.4	8.70	8.70	6.51	8.41
75	Yes	21.5	8.62	8.54	7.43	8.39

Table 3
Al species in water samples, aged 4 days.

Water sample	m/z (Da)	Relative peak intensity (%)	Al species
AC/EC-treated	75	55	$[Al(H_2O)_6 \cdot 1.54NaCl]^{3+}$
	84	100	$[Al(H_2O)_6 \cdot 2.00NaCl]^{3+}$
	93	60	$[Al_2(OH)_3(H_2O)_3 \cdot 2.05NaCl]^{3+}$
	148	11	$[Al_3(OH)_6(H_2O)_8 \cdot 2.00NaCl]^{3+}$
Supernatant	74	48	$[Al(H_2O)_6 \cdot 1.49NaCl]^{3+}$
	83	100	$[Al(H_2O)_6 \cdot 1.95NaCl]^{3+}$
	92	85	$[Al_2(OH)_3(H_2O)_3 \cdot 2.00NaCl]^{3+}$
	101	11	$[Al_3(OH)_6 \cdot 2.05NaCl]^{3+}$
	129	10	$[Al_3O(OH)_4(H_2O)_2 \cdot 3.18NaCl]^{3+}$
	156	11	$[Al_4O(OH)_7(H_2O)_2 \cdot 3.23NaCl]^{3+}$
	212	12	$[Al_5O_2(OH)_8(H_2O)_7 \cdot 3.54NaCl]^{3+}$

apparent. It should be noted that oxyhydroxo and hydroxo complexes incorporating NaCl were among the species identified by Sarpola et al. (2004).

It was unexpected to find "non-hydroxy" Al^{3+} in the AC/EC-treated water at pH ~8 (Table 3). While some proportion of this species, originally present in the freshly prepared sample, may have hydrolyzed during ageing, it was still a constituent of the aged sample. It could not have been formed from hydrolyzed species because of the high pH. Typically, hydrolyzed species age either to other hydrolyzed species (Tsai and Hsu, 1984) or to hydroxide precipitates (Smith, 1971).

The species with m/z of 148 Da in the AC/EC-treated water was not detected in the supernatant sample; it might have transformed to the species with m/z of 101. At the same time, the appearance of more complex, polynuclear, oxyhydroxoaluminum species in the supernatant can safely be imputed to ageing.

The samples, which had originally been prepared from water containing 200 mg/L NaCl, revealed only NaCl species, such as $Na(NaCl)_4^+$, $Na(NaCl)_{13}^+$ and $Na(NaCl)_{22}^+$, which obscured the Al species. Hence, samples were prepared from water containing 20 mg/L NaCl which allowed Al species to be detected. However, NaCl was still so pervasive as to associate with the Al complexes, presumably as Na^+Cl^- ion pairs in outer-sphere entities. It is noteworthy that species of the type, $Na(NaCl)_n^+$, were identified by Zhao et al. (2009).

3.6. Comparison of chemical coagulation and electrocoagulation

The settling behaviour of silica was enhanced by chemical coagulation over the range of Al dosages tested (Fig. 7). Both coagulants engendered a maximum initial settling rate of 5.6 cm/min, but aluminum chloride did so at ~25 mg/L Al, compared to ~30 mg/L for alum. The latter, however, tended to be the more effective; *i.e.*, alum achieved the higher initial settling rate at most of the dosages tested.

Interpolation of AC/EC test results indicated that the initial settling rate of 5.6 cm/min would result from AC/EC (2.1 A, 55 min). The aluminum dosage would amount to only 18.8 mg/L or 11.6% of the theoretical concentration, and significant energy loss as heat would result.

The chemical coagulation supernatants analyzed below the detection limit of 1 mg/L Al, while about 3 mg/L Al would be expected in the AC/EC supernatant. Hence, the adsorption mass ratios (mg Al/g silica) were calculated as follows: alum, 0.6; aluminum chloride, 0.5; and electrocoagulation, 0.3. Thus, the adsorption of aluminum amounting to 0.03% of the mass of silica in electrocoagulation effected the same initial settling rate as did aluminum from alum and aluminum chloride at 0.06% and 0.05%, respectively, of the mass of silica.

The quantity of the sediments increased with aluminum dosage. At the initial settling rate of 5.6 cm/min, the sediments produced by alum and aluminum chloride were 2.7 cm and 2.6 cm thick, respectively, compared to 2.1 cm for AC/EC (same cross-sectional area). That chemical coagulation produces more voluminous sediments than does electrocoagulation has been highlighted by Un et al. (2009), Yildiz et al. (2008), Barkley et al. (1993) and Vik et al. (1984). The differences in sediment volumes and adsorption mass ratios may be explained thus: chemical coagulation depends mainly on the precipitation of aluminum hydroxide in the sweep floc mechanism, whereas electrocoagulation depends mainly on the formation of complex aluminum species for interparticle bridging. Hence, chemical coagulation would require greater solid–liquid separation plant capacity than would electrocoagulation, for the same silica throughput.

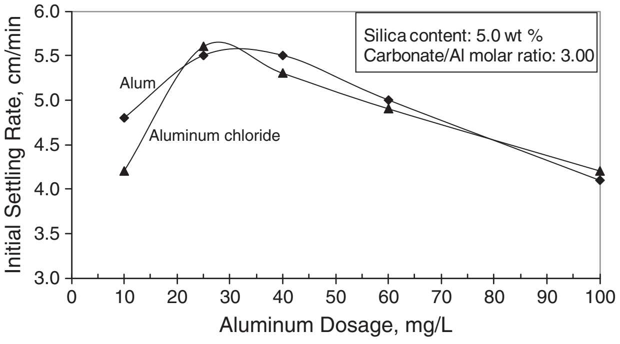

Fig. 7. Settling behaviour of chemically coagulated silica.

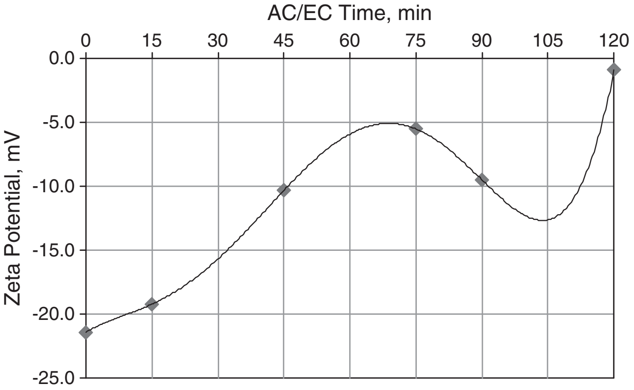

Fig. 8. Zeta potentials of electrocoagulated silica.

3.7. Effect of electrocoagulation on zeta potential

Fig. 8 shows how the zeta potential of silica changed with electrocoagulation time. From −21.4 mV in the as-received state (t = 0), the zeta potential decreased to −0.9 mV after 120 min of AC/EC treatment. In all cases, silica had been originally dispersed at 5.0 wt.% solids in feed water (de-ionized, 200 mg/L NaCl added) at pH 8.5. Agitation was applied continuously at an impeller tip speed of 1.73 m/s. It is noteworthy that, after 15 min of electrocoagulation, the zeta potential had decreased by only ~2 mV while the initial settling rate had been enhanced by over three orders of magnitude from 1.6×10^{-3} cm/min. The initial settling rate continued to increase linearly with electrocoagulation time. These results will be discussed in greater detail in another paper. They show that the destabilization of suspended particles can occur with hardly any measurable decrease of the zeta potential, when destabilization is effected by specific adsorption (Ofir et al., 2007).

Counter-ions are ions whose charge is opposite to that existing on the particle surface. It is considered that the zeta potential is reduced (as indicated by measurement) when counter-ions adsorb directly at charged sites on the particle surface (*i.e.*, electrostatic adsorption). From Fig. 8, therefore, it can be inferred that the complex aluminum ions may not be adsorbing preferentially at charged sites on the particle surface. Thus, the progress of specific adsorption (and, hence, of electrocoagulation dominated by specific adsorption) would not necessarily be indicated by lower measured zeta potential values. At this juncture, therefore, there appear to exist coagulation characteristics that are yet to be defined by further study, such as:

- whether there is any degree of order to adsorption;
- how adsorption sites are selected;
- whether aluminum speciation has any effect on order or selectivity;
- whether both types of adsorption (electrostatic and specific) occur simultaneously; and
- if so, to what extent does each occur and what conditions control the relative extents.

3.8. Controlling parameters

In this paper, we have seen how extending the electrocoagulation time caused the initial settling rate of silica to increase. The reason is that increasing AC/EC time increases the aluminum dosage, as would be the case if the current (or current density), for example, were increased. Hence, any parameter that controls aluminum dosage would influence the settling behaviour of silica. The effects of various parameters on electrocoagulation will be examined in subsequent papers.

4. Conclusions

The results of this work led to the following conclusions.

1. Agitation is beneficial, but not essential, to the effectiveness of AC/EC in enhancing the settling behaviour of fine silica.
2. Electrocoagulation for 75 min effected greater enhancement than did 30 min on the settling behaviour of silica.
3. Agitation shortened the electrocoagulation time required to enhance the settling behaviour of silica to a given degree.
4. In 30 min of AC/EC, the initial settling rate of silica was not greatly sensitive to agitation rate in the impeller tip speed range of 0 to 4.97 m/s. This result indicates that silica formed strong flocs.
5. The settling behaviour of fine particles is enhanced by their aggregation into flocs, as well as by direct adsorption onto large particles.
6. At a background concentration of 20 mg/L, NaCl was incorporated into all the cationic aluminum complexes that were identified. All the complexes were trivalent, and the molar ratio of NaCl:Al^{3+} decreased with increasing size of the oxyhydroxo complexes.
7. In the chemical coagulation tests, all of the added aluminum precipitated in the sweep floc mechanism. This was not the case with electrocoagulation, which produced less voluminous sediment for the same Al dosage.
8. In coagulation by specific adsorption, such as in electrocoagulation, zeta potential might not be a reliable indicator of the progress of coagulation.

Acknowledgments

The authors gratefully acknowledge the financial support provided by NSERC and Luscar Sterco for this work.

References

Akitt, J.W., Farthing, A., 1978. New ^{27}Al NMR studies of the hydrolysis of the aluminum (III) cation. J. Magn. Reson. 32, 345–352.

American Water Works Association, 1977. Simplified Procedures for Water Examination: AWWA manual M12. AWWA, pp. 68–78.

Amirtharajah, A., O'Melia, C.R., 1990. Coagulation processes: destabilization, mixing, and flocculation, In: Pontius, F.W. (Ed.), Water Quality and Treatment, fourth ed. McGraw-Hill, Inc., New York, pp. 269–365.

ASTM, 1996. Annual Book of ASTM Standards, Volume 05.01. American Society for Testing and Materials, Philadelphia, PA.

ASTM, 1997. Annual Book of ASTM Standards, Volume 04.08. American Society for Testing and Materials, Philadelphia, PA.

Baes, C.F., Mesmer, R.E., 1976. The Hydrolysis of Cations. John Wiley & Sons, New York.

Barkley, N.P., Farrell, C.W., Gardner-Clayson, T.W., 1993. Alternating current electrocoagulation for Superfund site remediation. J. Air Waste Manage. Assoc. 43, 784–789.

Black, A.P., 1967. Electrokinetic characteristics of hydrous oxides of aluminum and iron. In: Faust, S.D., Hunter, J.V. (Eds.), Principles and Applications of Water Chemistry. John Wiley & Sons, Inc., New York, pp. 274–300.

Bouyer, D., Coufort, C., Liné, A., Zdravka, D.-Q., 2005. Experimental analysis of floc size distributions in a 1-L jar under different hydrodynamics and physicochemical conditions. J. Colloid Interface Sci. 292, 413–428.

Cañizares, P., Martínez, F., Jiménez, C., Lobato, J., Rodrigo, M.A., 2006. Comparison of the aluminum speciation in chemical and electrochemical dosing processes. Ind. Eng. Chem. Res. 45, 8749–8756.

Cohen, J.M., Hannah, S.A., 1971. Coagulation and flocculation, Water Quality and Treatment — A Handbook of Public Water Supplies, third ed. McGraw-Hill Book Company, New York, pp. 66–122.

Coufort, C., Bouyer, D., Liné, A., 2005. Flocculation related to local hydrodynamics in a Taylor–Couette reactor and in a jar. Chem. Eng. Sci. 60, 2179–2192.

Dentel, S.K., Gossett, J.M., 1988. Mechanisms of coagulation with aluminum salts. J. Am. Water Works Assn. 80, 187–198.

Duan, J., Gregory, J., 2003. Coagulation by hydrolysing metal salts. Adv. Colloid Interface Sci. 100–102, 475–502.

Elzo, D., Huisman, I., Middelink, E., Gekas, V., 1998. Charge effects on inorganic membrane performance in a cross-flow microfiltration process. Colloids Surf. A 138, 145–159.

Hahn, H.H., Stumm, W., 1968. Coagulation of Al(III). The role of adsorption of hydrolyzed aluminum in the kinetics of coagulation. In: Gould, R.F. (Ed.), Adsorption from Aqueous Solution. Advances in Chemistry Series, 79. American Chemical Society, Washington, DC, pp. 91–111.

Huang, C.P., 1981. The surface acidity of hydrous solids. In: Anderson, M.A., Rubin, A.J. (Eds.), Adsorption of Inorganics at Solid–Liquid Interfaces. Ann Arbor Science Publishers Inc., Ann Arbor, MI, pp. 183–218.

Hunt, J.P., 1965. Metal Ions in Aqueous Solution. W.A. Benjamin, Inc., New York, pp. 45–54.

Hunter, R.J., 1981. Zeta Potential in Colloid Science. Academic Press, London, pp. 132–344.

Jenke, D.R., Diebold, F.E., 1984. Electroprecipitation treatment of acid mine wastewater. Water Res. 18, 855–859.

Letterman, R.D., Vanderbrook, S.G., Sricharoenchaikit, P., 1982. Electrophoretic mobility measurements in coagulation with aluminum salts. J. Am. Water Works Assn. 74, 44–51.

Lyklema, J., 1978. Surface chemistry of colloids in connection with stability. In: Ives, K.J. (Ed.), The Scientific Basis of Flocculation. Sijthoff & Noordhoff, The Netherlands, pp. 1–36.

Masliyah, J.H., 1994. Electrokinetic Transport Phenomena. AOSTRA Technical Publication Series #12, Edmonton, Canada.

Montgomery, J.M., Consulting Engineers, Inc., 1985. Water Treatment Principles and Design. John Wiley & Sons, New York.

Ofir, E., Oren, Y., Adin, A., 2007. Electroflocculation: the effect of zeta potential on particle size. Desalination 204, 33–38.

Parekh, B.K., Groppo, J.G., Justice, J.G., 1992. Removal of fine particulates and metal ions from process discharge waste water using AC electrocoagulation technique. In: Chander, S. (Ed.), Emerging Process Technologies for a Cleaner Environment. AIME Proceedings, Phoenix, Arizona, pp. 99–105.

Parthasarathy, N., Buffle, J., 1985. Study of polymeric aluminium (III) hydroxide solutions for application in waste water treatment. Properties of the polymer and optimal conditions of preparation. Water Res. 19, 25–36.

Pretorius, W.A., Johannes, W.G., Lempert, G.G., 1991. Electrolytic iron flocculant production with a bipolar electrode in series arrangement. Water SA 17, 133–138.

Rank, Brothers, 1986. Operating Instructions and Manual for the Particle Microelectrophoresis Apparatus Mark II. Rank Brothers, Cambridge, England.

Riddick, T.M., 1968. Control of Colloid Stability through Zeta Potential, vol. I. Livingston Publishing Company, Wynnewood, Pennsylvania, pp. 21–24.

Sarpola, A., Hietapelto, V., Jalonen, J., Jokela, J., Laitinen, R.S., 2004. Identification of the hydrolysis products of $AlCl_3 \cdot 6H_2O$ by electrospray ionization mass spectrometry. J. Mass Spectrom. 39, 423–430.

Sarpola, A.T., Hietapelto, V.K., Jalonen, J.E., Jokela, J., Rämö, J.H., 2006. Comparison of hydrolysis products of $AlCl_3 \cdot 6H_2O$ in different concentrations by electrospray ionization time of flight mass spectrometer (ESI TOF MS). Int. J. Environ. Anal. Chem. 86, 1007–1018.

Sharma, S.K., Stanley, D.A., Harris, J., 1994. Determining the effect of physicochemical parameters on floc size using a population balance model. Miner. Metall. Process. 11, 168–173.

Smith, R.W., 1971. Relations among equilibrium and nonequilibrium aqueous species of aluminum hydroxyl complexes. In: Gould, R.F. (Ed.), Nonequilibrium Systems in Natural Water Chemistry, Advances in Chemistry Series 106. American Chemical Society, Washington, DC, pp. 250–279.

Snoeyink, V.L., Jenkins, D., 1980. Water Chemistry. John Wiley & Sons, New York, p. 213.

Spears, D.R., Stanley, D.A., 1994. Study of shear-flocculation of silica. Miner. Metall. Process. 11, 5–11.

Stol, R.J., van Helden, A.K., de Bruyn, P.L., 1976. Hydrolysis-precipitation studies of aluminum(III) solutions: 2. A kinetic study and model. J. Colloid Interface Sci. 57, 115–131.

Stumm, W., 1992. Chemistry of the Solid–Water Interface. Wiley-Interscience, New York.

Stumm, W., Morgan, J.J., 1970. Aquatic Chemistry. Wiley-Interscience, New York.

Stumm, W., O'Melia, C.R., 1968. Stoichiometry of coagulation. J. Am. Water Works Assn. 60, 514–539.

Tambo, N., 1991. Basic concepts and innovative turn of coagulation/flocculation. Water Supply 9, 1–10 Jönköping.

Trompette, J.L., Vergnes, H., 2009. On the crucial influence of some supporting electrolytes during electrocoagulation in the presence of aluminum electrodes. J. Hazard. Mater. 163, 1282–1288.

Tsai, P.P., Hsu, P.H., 1984. Studies of aged OH-Al solutions using kinetics of Al-ferron reactions and sulfate precipitation. Soil Sci. Soc. Am. J. 48, 59–65.

Un, U.T., Koparal, A.S., Ogutveren, U.B., 2009. Electrocoagulation of vegetable oil refinery wastewater using aluminum electrodes. J. Environ. Manage. 90, 428–433.

Vik, E.A., Carlson, D.A., Eikum, A.S., Gjessing, E.T., 1984. Electrocoagulation of potable water. Water Res. 18, 1355–1360.

Warren, L.J., 1975. Shear-flocculation of ultrafine scheelite in sodium oleate solutions. J. Colloid Interface Sci. 50, 307–318.

Yildiz, Y.S., Koparal, A.S., Keskinler, B., 2008. Effect of initial pH and supporting electrolyte on the treatment of water containing high concentration of humic substances by electrocoagulation. Chem. Eng. J. 138, 63–72.

Zhao, H., Liu, H., Qu, J., 2009. Effect of pH on the aluminum salts hydrolysis during coagulation process: formation and decomposition of polymeric aluminum species. J. Colloid Interface Sci. 330, 105–112.